Cell Reports

Report

Oocyte Factors Suppress Mitochondrial Polynucleotide Phosphorylase to Remodel the Metabolome and Enhance Reprogramming

Graphical Abstract

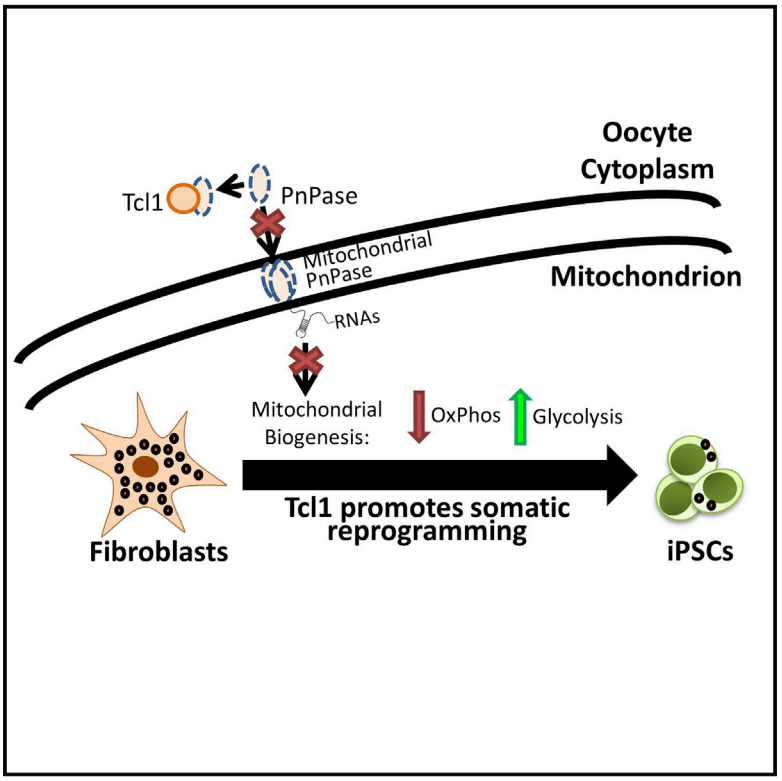

Authors

Swea-Ling Khaw, Chua Min-Wen, Cheng-Gee Koh, Bing Lim, Ng Shyh-Chang

Correspondence

cgkoh@ntu.edu.sg (C.-G.K.), ngsc1@gis.a-star.edu.sg (N.S.-C.)

In Brief

Khaw et al. identify the oocyte Tcl1-PnPase pathway as a critical mitochondrial switch during reprogramming into iPSCs. They find that Tcl1 suppresses the mitochondrial localization of PNPase, thus inhibiting mitochondrial biogenesis and oxidation phosphorylation.

Highlights

- Oocyte-enriched Tcl1 enhances the efficiency and quality of somatic reprogramming
- Tcl1b1 promotes Akt phosphorylation to promote somatic reprogramming
- Tcl1 suppresses mitochondrial biogenesis via PnPase to promote somatic reprogramming
- The Tcl1-PnPase switch remodels the metabolome to enhance somatic reprogramming

Khaw et al., 2015, Cell Reports *12*, 1080–1088
August 18, 2015
http://dx.doi.org/10.1016/j.celrep.2015.07.032

CellPress

OPEN ACCESS
CellPress

Cell Reports
Report

Oocyte Factors Suppress Mitochondrial Polynucleotide Phosphorylase to Remodel the Metabolome and Enhance Reprogramming

Swea-Ling Khaw,[1,2] Chua Min-Wen,[1] Cheng-Gee Koh,[2,3,*] Bing Lim,[1] and Ng Shyh-Chang[1,*]
[1]Stem Cell and Regenerative Biology, Genome Institute of Singapore, Singapore 138672, Singapore
[2]School of Biological Sciences, Nanyang Technological University, Singapore 637551, Singapore
[3]Mechanobiology Institute, National University of Singapore, Singapore 117411, Singapore
*Correspondence: cgkoh@ntu.edu.sg (C.-G.K.), ngsc1@gis.a-star.edu.sg (N.S.-C.)
http://dx.doi.org/10.1016/j.celrep.2015.07.032

SUMMARY

Oocyte factors not only drive somatic cell nuclear transfer reprogramming but also augment the efficiency and quality of induced pluripotent stem cell (iPSC) reprogramming. Here, we show that the oocyte-enriched factors Tcl1 and Tcl1b1 significantly enhance reprogramming efficiency. Clonal analysis of pluripotency biomarkers further show that the Tcl1 oocyte factors improve the quality of reprogramming. Mechanistically, we find that the enhancement effect of Tcl1b1 depends on Akt, one of its putative targets. In contrast, Tcl1 suppresses the mitochondrial polynucleotide phosphorylase (PnPase) to promote reprogramming. Knockdown of PnPase rescues the inhibitory effect from *Tcl1* knockdown during reprogramming, whereas PnPase overexpression abrogates the enhancement from *Tcl1* overexpression. We further demonstrate that Tcl1 suppresses PnPase's mitochondrial localization to inhibit mitochondrial biogenesis and oxidation phosphorylation, thus remodeling the metabolome. Hence, we identified the Tcl1-PnPase pathway as a critical mitochondrial switch during reprogramming.

INTRODUCTION

Somatic cell nuclear transfer (SCNT) was the first nuclear reprogramming method to be developed. In this method, a somatic nucleus is rapidly reprogrammed by oocyte cytosolic factors to gain pluripotency in a deterministic manner (Brambrink et al., 2006). The cells generated from SCNT are bona fide pluripotent stem cells, more similar to embryonic stem cells (ESCs) derived from the fertilization of oocytes by spermatozoa than regular induced pluripotent stem cells (iPSCs) (Stadtfeld and Hochedlinger, 2010). However, while SCNT is conceptually straightforward, its application has been hindered by logistical difficulties and ethical controversies, especially in humans. The advent of transcription-factor-mediated iPSC reprogramming (Takahashi and Yamanaka, 2006) represented a significant step toward generating patient-specific stem cells that can be used for autologous cell replacement therapy and establishment of disease models. Compared to SCNT, this method is technically simple and free of logistical constraints and ethical concerns with human blastocyst destruction. Furthermore, it has revealed important insights into the molecular mechanisms of reprogramming and pluripotency.

Its only drawback is that it is less efficient at establishing complete, bona fide pluripotency than SCNT (Le et al., 2014). Therefore, it is conceivable that some oocyte cytosolic factors might work synergistically with the Oct4, Sox2, Klf4, and c-Myc nuclear transcription factors to enhance iPSC reprogramming. However, while many transcription factors have been shown to enhance the generation of iPSCs, the majority of oocyte factors remain poorly investigated.

The mammalian oocyte-enriched T-cell leukemia (Tcl1) protein family consists of cytosolic, non-enzymatic proteins that are known to bind the Akt kinase, among other targets (Laine et al., 2000). Here, we show that Tcl1 and its closely related homolog Tcl1b1 significantly boost the somatic reprogramming of fibroblasts. Tcl1b1 promotes Akt activation to promote reprogramming, whereas Tcl1 suppresses mitochondrial biogenesis via PnPase to remodel the metabolome, thereby providing the cytoplasmic milieu to enhance somatic reprogramming.

RESULTS

Oocyte Tcl1 and Tcl1b1 Enhance Reprogramming of Fibroblasts

We screened 20 oocyte-enriched genes, selected based on their abundance in ESCs and oocytes (Wang et al., 2010b; Zhang et al., 2009), by testing their effects on iPSC reprogramming of mouse fibroblasts using retroviral *Oct4, Sox2*, and *Klf4* (OSK; Figures S1A and S1B). Out of the 20 oocyte-enriched genes, only *Tcl1* and *Tcl1b1* significantly increased the number of alkaline phosphatase (AP)-positive iPSC colonies (Figure 1A). Endogenous *Tcl1* expression is similar to *Nanog* in that it is highly upregulated only at the late stage of iPSC reprogramming, when cells begin to acquire pluripotency (Figure 1B), whereas endogenous *Tcl1b1* is undetectable throughout iPSC reprogramming.

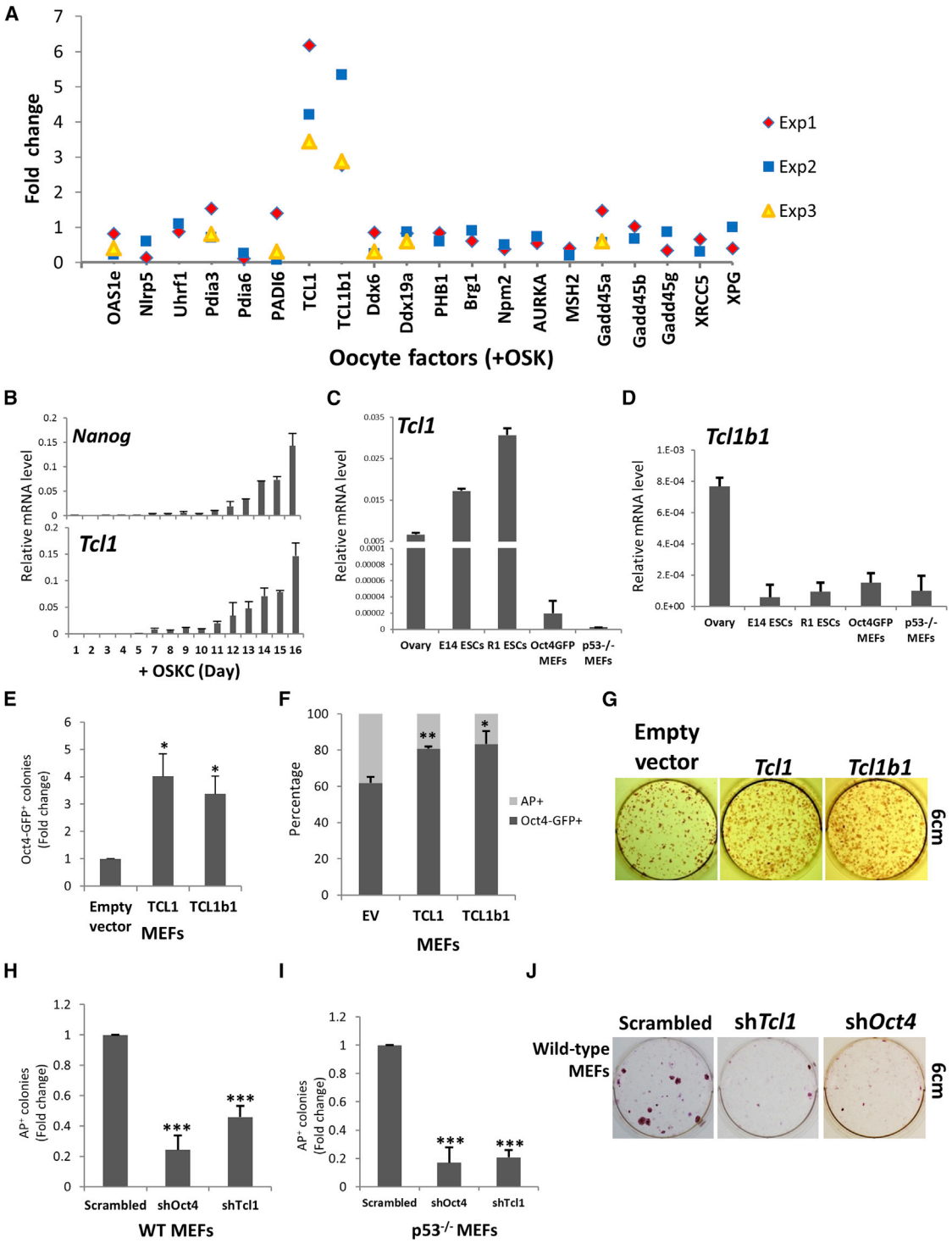

Figure 1. Overexpression of *Tcl1* and *Tcl1b1* Enhance Somatic Reprogramming

(A) Fold change in AP-positive colonies after OSK-mediated reprogramming of WT MEFs in a mini-screen against oocyte-enriched genes, relative to empty vector (EV) control.

(B) Gene expression of endogenous *Nanog* and *Tcl1* during the time course of iPSC reprogramming of MEFs.

(C and D) Gene expression of (C) *Tcl1* and (D) *Tcl1b1* in the ovary, two ESCs, and two MEF lines.

(E) Fold change in *Oct4*-GFP^{+} colonies after *Tcl1* and *Tcl1b1* overexpression during OSK reprogramming of WT MEFs.

(F) Percentage of AP+ colonies that are *Oct4*-GFP^{+} after *Tcl1* and *Tcl1b1* overexpression during OSK reprogramming of WT MEFs.

(legend continued on next page)

Furthermore, *Tcl1* is expressed highly in both mouse oocytes and ESCs (Figure 1C), whereas *Tcl1b1* is expressed only in oocytes (Figure 1D), consistent with previous findings (Hallas et al., 1999). These data support their candidacy as oocyte reprogramming factors.

To validate our initial screen results, we repeated *Tcl1* and *Tcl1b1* overexpression during reprogramming of *Oct4*-GFP mouse embryonic fibroblasts (MEFs) and found that both *Tcl1* factors could significantly increase *Oct4*-GFP$^+$ colonies (Figure 1E). *Tcl1* and *Tcl1b1* overexpression also significantly increased the percentage of *Oct4*-GFP$^+$ colonies within AP+ colonies (Figure 1F). This enhancement was independent of *c-Myc* overexpression (Figure 1G) and *p53* deletion (Figure S1C).

Conversely, somatic reprogramming efficiency was significantly impaired by the knockdown of endogenous *Tcl1* (Figure S1D) during iPSC reprogramming of either wild-type (WT) or *p53*$^{-/-}$ MEFs (Figures 1H–1J), thus highlighting its necessity in somatic reprogramming. Taken together, these observations suggest that the Tcl1 oocyte factors represent a distinct pathway critical to reprogramming.

Oocyte Tcl1 and Tcl1b1 Enhance Pluripotency Biomarkers after iPSC Derivation

Recent studies have suggested that other biomarkers, besides *Oct4*-GFP fluorescence, can support the assessment of bona fide iPSC reprogramming efficiency (Buganim et al., 2012; Golipour et al., 2012). Therefore, we used a single-clone profiling assay with nanofluidic chips to profile *Tbx3, Nanog*, and the imprinted *Dlk1-Dio3* gene cluster as biomarkers for iPSC quality (Figure S2A), as these biomarkers had been shown to predict bona fide pluripotency and differentiation potency (Han et al., 2010; Niwa et al., 2009; Silva et al., 2009; Stadtfeld and Hochedlinger, 2010). Our analysis revealed that *Nanog*, *Tbx3*, *Gtl-2*, and *Rian* were upregulated to pluripotent ESC-like levels in *Tcl1*- and *Tcl1b1*-expressing clones, in contrast to OSK-only or partially reprogrammed iPSCs (Figures S2B–S2E), whereas *Dlk-1*, which is imprinted and anti-correlated with pluripotency, was downregulated to ESC-like levels in *Tcl1*- and *Tcl1b1*-expressing clones (Figure S2F). In total, either *Tcl1* or *Tcl1b1* overexpression could enhance reprogramming to the ESC-like state (Figure S2G) with ~50% efficiency among *Oct4*-GFP+ colonies, whereas OSK-only could produce ESC-like colonies with only 10% efficiency (Figure S2H). This further supports our findings that *Tcl1* and *Tcl1b1* enhance iPSC reprogramming.

Tcl1b1 Enhances Somatic Reprogramming by Increasing Akt Activity

Next, we investigated the molecular mechanism for *Tcl1*- and *Tcl1b1*-mediated enhancement of somatic reprogramming. Since both Tcl1 and Tcl1b1 are known Akt1/2 cofactors (Laine et al., 2000), we explored the role of Akt during reprogramming. Although Akt1 can stimulate heterokaryon and iPSC reprogramming, Akt's role in SCNT reprogramming had remained unclear (Nakamura et al., 2008; Zhu et al., 2010). We observed a gradual increase in phospho-Akt during iPSC reprogramming by OSK factors (Figure 2A), and Akt was predominantly phosphorylated in ESCs relative to MEFs (Figure 2B). The pro-reprogramming role of Akt was confirmed when ectopic Akt1 increased reprogramming efficiency (Figure S3A), whereas inhibition of endogenous Akt activity suppressed iPSC reprogramming (Figure S3B). When we compared reprogramming using OSK factors alone, or OSK factors with either *Tcl1* or *Tcl1b1* overexpression, we found that only ectopic *Tcl1b1* increased Akt phosphorylation far above the level achieved by OSK factors alone (Figure 2C). This suggests that only *Tcl1b1*, but not *Tcl1*, significantly enhances Akt activation.

To test whether *Tcl1* and *Tcl1b1* act through Akt activation to promote iPSC reprogramming, we sought to verify whether pharmacological inhibition of Akt1/2 might specifically abrogate *Tcl1*'s and *Tcl1b1*'s enhancement of iPSC reprogramming. Although Akt1/2 inhibition abrogated *Tcl1b1*'s enhancement of iPSC reprogramming (Figure 2D), Akt1/2 inhibition failed to abrogate the 3-fold enhancement promoted by *Tcl1* (Figure 2E). A different Akt1/2 inhibitor yielded similar results (Figure S3C). On the other hand, co-overexpression of both *Tcl1* and *Tcl1b1* together synergistically increased reprogramming efficiency more than expected (Figure 2F), implying that *Tcl1*'s enhancement mechanism does not completely overlap with that of *Tcl1b1* and that another mechanistic target besides Akt exists downstream of *Tcl1* for reprogramming (Figure 2G).

Tcl1 Promotes Reprogramming by Suppressing Mitochondrial PnPase

To identify this other mechanistic target of Tcl1 in reprogramming, we performed co-immunoprecipitation (coIP) experiments in MEFs expressing hemagglutinin (HA)-tagged Tcl1 (*HA-Tcl1*), with and without the OSK reprogramming factors. We readily identified endogenous Pnpt1 as Tcl1's main binding partner (Figure 3A). *Pnpt1* encodes mitochondrial polynucleotide phosphorylase (PnPase), an RNA-binding protein that plays an important role in RNA import and processing in mitochondria and, thus, mitochondrial homeostasis (Chen et al., 2006; Wang et al., 2010a). When we overexpressed *Tcl1*, the mitochondrial fraction of endogenous PnPase was significantly reduced but not the total pool of PnPase (Figures 3B and 3C). This suggested that Tcl1 suppressed the mitochondrial localization—and, thus, the mitochondrial activity—of PnPase.

Furthermore, we discovered that overexpression of *Pnpt1* (Figure S4A) significantly suppressed somatic reprogramming by 60% (Figure 3D), whereas knockdown of the *Pnpt1* gene with two independent small hairpin RNAs (shRNAs) (Figure S4B)

(G) Fold change in AP+ colonies after Tet-inducible *Tcl1* and *Tcl1b1* overexpression during OSK + *c-Myc* reprogramming of MEFs.
(H and I) Fold change in AP+ colonies after *Tcl1* and *Tcl1b1* shRNA knockdown during OSK reprogramming of (H) WT MEFs and (I) *p53*$^{-/-}$ MEFs, relative to scrambled shRNA and sh*Oct4*.
(J) Images of AP-stained colonies quantified in (H).
All data are shown as the mean ± SEM of three biological replicates. *$p < 0.05$; **$p < 0.01$; ***$p < 0.001$; n.s., not significant. See also Figures S1 and S2 and Tables S1 and S2.

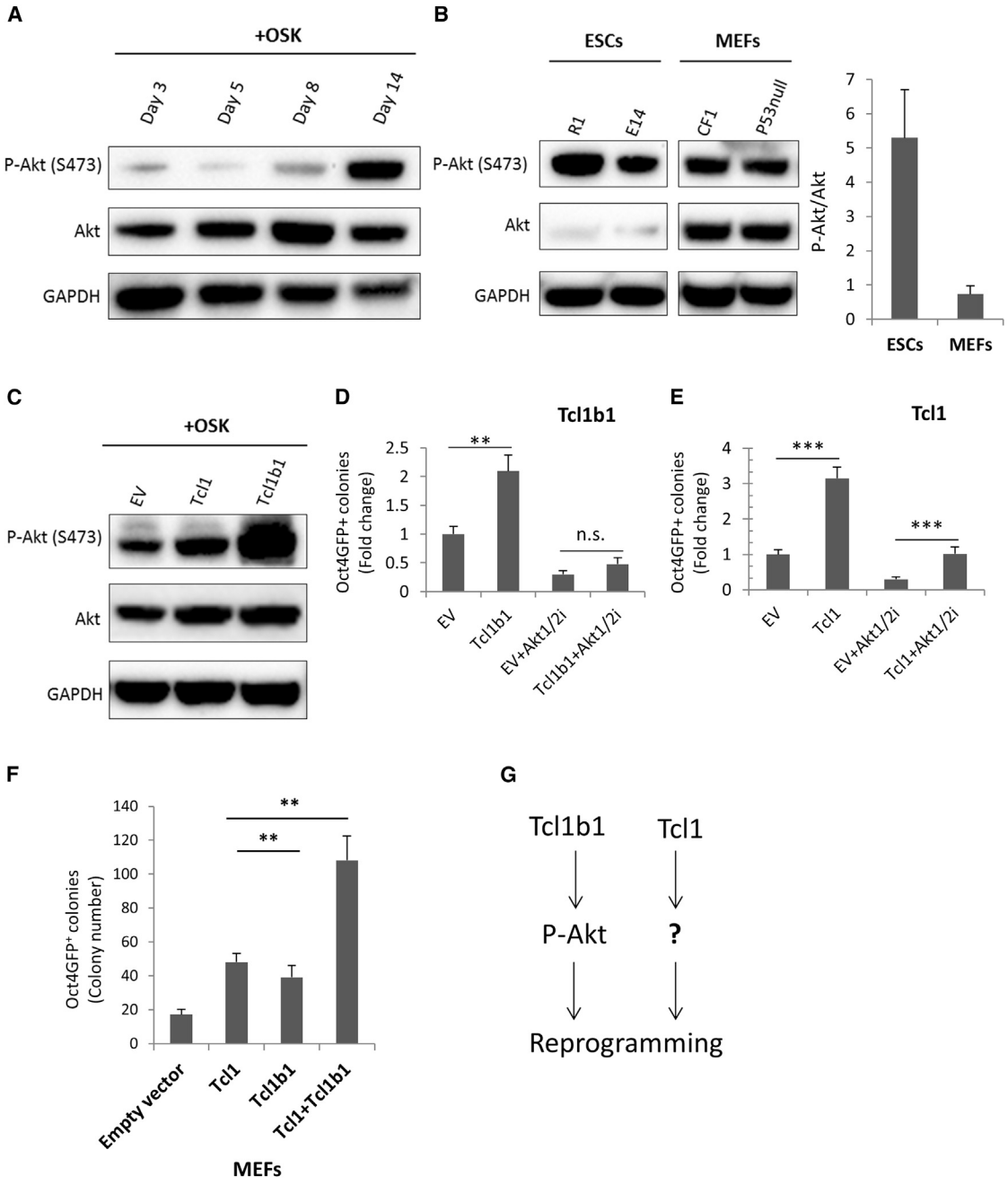

Figure 2. Tcl1b1 Promotes Akt Phosphorylation to Enhance iPSC Reprogramming

(A) Abundance of phospho-Akt (Ser473) protein during the time course of iPSC reprogramming of WT MEFs.

(B) Abundance of phospho-Akt (Ser473) protein and densitometric quantification of phospho-Akt relative to total Akt (pAkt/tAkt) in mouse ESCs and MEFs. GAPDH served as the total protein loading control.

(C) Abundance of phospho-Akt (Ser473) protein after *Tcl1* and *Tcl1b1* overexpression during OSK-mediated reprogramming of WT MEFs.

(D and E) Fold change in *Oct4*-GFP$^+$ colonies after (D) *Tcl1b1* and (E) *Tcl1* overexpression during OSK-mediated reprogramming of WT MEFs, with or without Akt1/2 inhibitor (Akt1/2i).

(F) Fold change in *Oct4*-GFP$^+$ colonies after double co-overexpression of *Tcl1* and *Tcl1b1* during OSK-mediated reprogramming of WT MEFs.

(G) Diagram model depicting how *Tcl1* and *Tcl1b1-Akt* regulate somatic reprogramming.

All data are shown as the mean ± SEM of at least three biological replicates. *$p < 0.05$; **$p < 0.01$; ***$p < 0.001$. See also Figure S3.

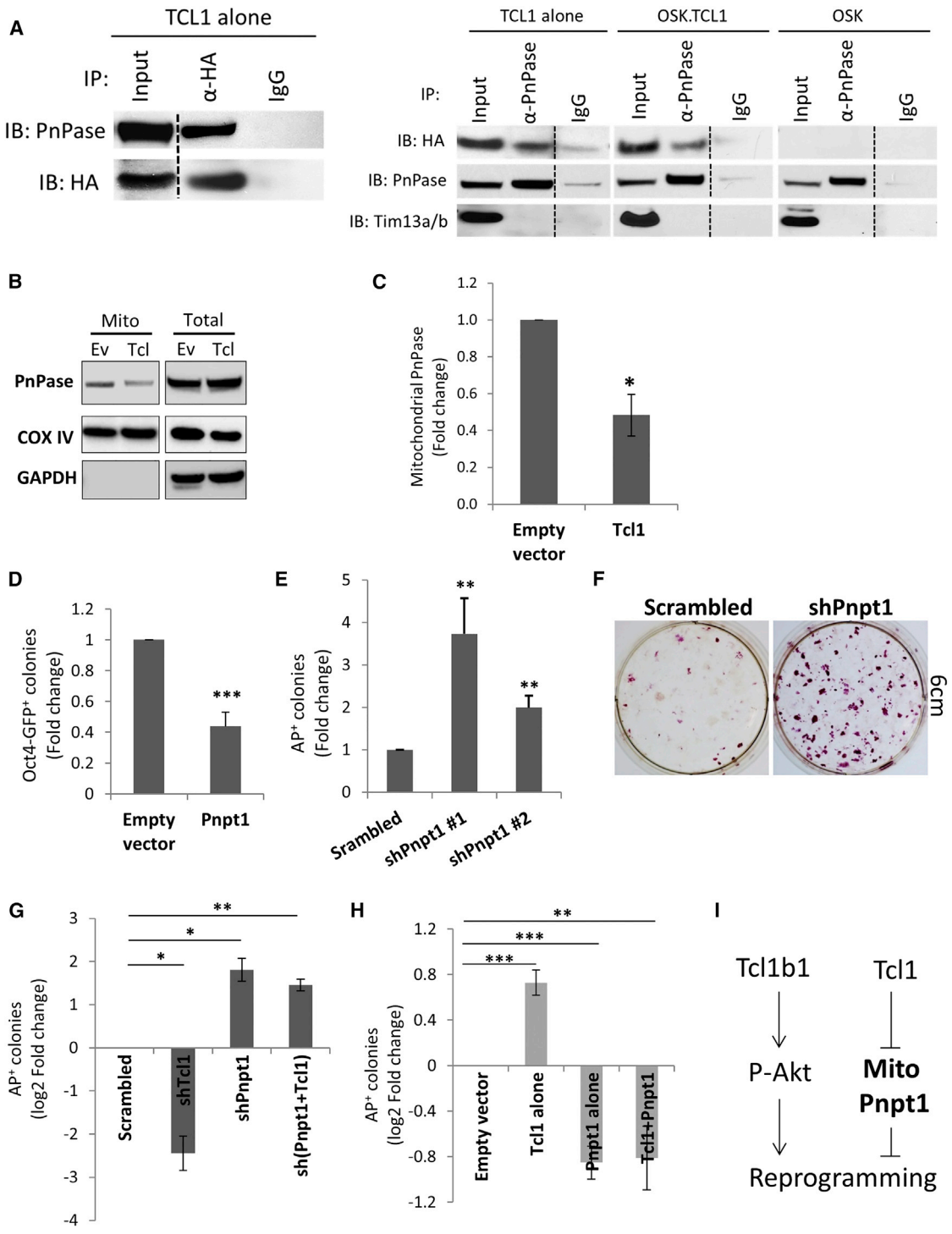

Figure 3. Tcl1 Suppresses Mitochondrial PnPase to Enhance iPSC Reprogramming

(A) Western blots of coIPs (IP) between ectopic HA-Tcl1 and endogenous PnPase, immunoblotted (IB) with anti-HA or anti-PnPase. Tim13a/b is a mitochondrial inner membrane protein and served as a negative control. Three experiments were performed with similar results. IgG, immunoglobulin G.

(B) PnPase protein in mitochondrial fraction (Mito) and total protein (Total) pools. COX IV served as the mitochondrial loading control, while GAPDH served as the total protein loading control. EV, empty vector.

(C) Densitometric quantification of mitochondrial PnPase protein, relative to mitochondrial COX IV loading control. Three biological replicates were quantified.

(D) Fold change in *Oct4*-GFP$^+$ colonies after *Pnpt1* overexpression during OSK-mediated reprogramming of WT MEFs.

(E) Fold change in *Oct4*-GFP$^+$ colonies after *Pnpt1* shRNA knockdown during OSK reprogramming of WT MEFs.

(legend continued on next page)

significantly enhanced iPSC reprogramming by ~4-fold (Figures 3E and 3F). This enhancement was similar in magnitude to *p53* knockdown (Figure S4C), but it was even further enhanced to ~12-fold by *p53* deletion (Figure S4D), suggesting that *Pnpt1* depletion also works independently of *p53* depletion. Thus, mitochondrial PnPase does inhibit iPSC reprogramming, independently of the p53 pathway and its effects on cellular proliferation and apoptosis.

To validate whether *Pnpt1* functions downstream of *Tcl1* during reprogramming, we performed genetic epistasis experiments. We found that *Pnpt1* knockdown fully rescued the inhibitory effect of *Tcl1* knockdown during reprogramming (Figure 3G). On the other hand, *Pnpt1* overexpression fully abrogated the enhancement effect of *Tcl1* during reprogramming (Figure 3H). These data prove that mitochondrial *Pnpt1* functions downstream of *Tcl1* in reprogramming (Figure 3I).

Tcl1-PnPase Pathway Reprograms the Cellular Metabolome

While somatic cells depend mostly on mitochondrial oxidative phosphorylation (OxPhos), pluripotent stem cells possess immature mitochondria and preferentially use glycolysis as their major source of energy (Prigione et al., 2010; Folmes et al., 2011). Although this preference has been well characterized in ESCs, the pluripotency or oocyte factors responsible for this metabolic switch during somatic reprogramming had remained incompletely resolved. To test whether the Tcl1-Pnpt1 switch regulates somatic reprogramming by regulating mitochondrial homeostasis, we first examined the effects of Tcl1-Pnpt1 on mtDNA levels as an indicator of mitochondrial replication and biogenesis. *Pnpt1*-mediated import of nucleus-encoded RNAs—including *MRP* and *RNase P* RNAs, tRNAs, and *5S* rRNA—is thought to be essential for mtDNA replication and gene expression (Wang et al., 2010a). Interestingly, we found that *Tcl1* suppressed mtDNA by 30%, whereas *Pnpt1* increased it by 50% (Figure 4A). Moreover, *Pnpt1* overexpression overwrote the effects of *Tcl1* overexpression (Figure 4A), proving that it lies downstream of *Tcl1* in regulating mitochondrial biogenesis.

To understand the roles of mitochondrial Pnpt1 and Tcl1 in regulating cellular metabolism, we profiled the metabolomes of WT MEFs overexpressing either *Tcl1* or *Pnpt1*, using a liquid chromatography-tandem mass spectrometry (LC-MS/MS) platform. We observed that *Tcl1* and *Pnpt1* overexpression transformed significant segments of the metabolome in opposite directions, relative to the empty vector control (Figure 4B). In the glycolysis pathway, *Tcl1* significantly increased fructose-1,6-bisphosphate (F-1,6-BP), suggesting higher phosphofructokinase (PFK) flux than the control, whereas *Pnpt1* significantly decreased F-1,6-BP, suggesting lower PFK flux than the control (Figure 4C). PFK is the major rate-limiting irreversible step in glycolysis. Thus, *Tcl1* increased input flux into glycolysis, whereas *Pnpt1* decreased input flux into glycolysis, which is also evident from the significantly lower levels of glycolytic intermediates from G3P to PEP (Figure 4C). At the final irreversible step of pyruvate kinase (PK) in glycolysis, which controls the glycolytic outflows, *Tcl1* and *Pnpt1* again show opposite trends. *Tcl1* significantly increased phosphoenolpyruvate (PEP) and decreased pyruvate, whereas *Pnpt1* caused opposite changes (Figure 4C), suggesting that *Tcl1* decreased PK flux to promote the accumulation of glycolytic intermediates for growth, whereas *Pnpt1* increased PK flux to feed pyruvate into mitochondrial OxPhos. These are supported by observations that *Tcl1* increased the glycolysis-derived D-glucono-δ-lactone-6-phosphate (Figure 4D), which shunts into the pentose phosphate pathway for nucleotide synthesis, whereas *Pnpt1* increased the ATP/AMP ratio (Figure 4E) and decreased the glutathione GSH/GSSG ratio (Figure 4F), indicating that *Pnpt1* promoted mitochondrial OxPhos and ROS production.

To prove that these metabolic effects of *Tc1* and *Pnpt1* are relevant to reprogramming and pluripotency, we imaged and measured the mitochondrial membrane potential ($\Delta\psi_m$) of ESCs and MEFs undergoing OSK reprogramming (Figure 4G). Previous studies had shown that a high $\Delta\psi_m$ can result from a preference for glycolysis and a lower rate of respiration, leading to a slower dissipation of the mitochondrial membrane potential (Fantin et al., 2006; Yoshida et al., 2009). Using a live $\Delta\psi_m$ probe, we performed flow cytometry analysis on live cells and found that *Tcl1* significantly increased the proportion of ESC-like $\Delta\psi_m^{HIGH}$ cells during OSK reprogramming (Figure 4H). Similarly, *Pnpt1* knockdown significantly increased the proportion of ESC-like $\Delta\psi_m^{HIGH}$ cells during reprogramming (Figure 4I).

To confirm these metabolic observations, we examined the bioenergetics profiles of MEFs by measuring the mitochondrial oxygen consumption rate (OCR) to assay respiration rates and by measuring the extracellular acidification rate (ECAR) to assay glycolytic rates. Relative to the scrambled control, we observed that *Pnpt1* was required for normal basal and maximal respiration after *Pnpt1* knockdown (Figure 4J). On the other hand, *Pnpt1* knockdown increased the basal glycolysis rate, suggesting that Pnpt1 suppressed glycolysis (Figure 4J). Similarly, *Tcl1* overexpression decreased basal respiration and maximal respiration by 40% (Figure 4K). Furthermore *Tcl1* overexpression increased the glycolytic rate by 40%–60% (Figure 4K), similar to *Pnpt1* knockdown. Most importantly, we found that *Pnpt1* overexpression could rescue not only *Tcl1*'s inhibition of respiration (Figure 4L) but also *Tcl1*'s enhancement of glycolytic flux (Figure 4M), confirming that *Pnpt1* acts downstream of *Tcl1* in metabolic reprogramming.

DISCUSSION

Our results contribute to solving a long-standing mystery of how oocyte-enriched cytosolic factors facilitate reprogramming (Gurdon and Melton, 2008). In this study, we demonstrated that

(F) Images of AP-stained colonies after *Pnpt1* shRNA knockdown during OSK reprogramming of WT MEFs.
(G and H) Log_2 (fold change) in *Oct4*-GFP$^+$ colonies after (G) double shRNA knockdown or (H) double co-overexpression of *Tcl1* and *Pnpt1* during OSK reprogramming of WT MEFs. Fold changes were plotted in log_2 scale to capture both the efficiency gains and losses adequately.
(I) Diagram model depicting how *Tcl1-Pnpt1* and *Tcl1b1-Akt* regulate somatic reprogramming.
All data are shown as the mean ± SEM of at least three biological replicates. *$p < 0.05$; **$p < 0.01$; ***$p < 0.001$. See also Figure S4 and Tables S1 and S2.

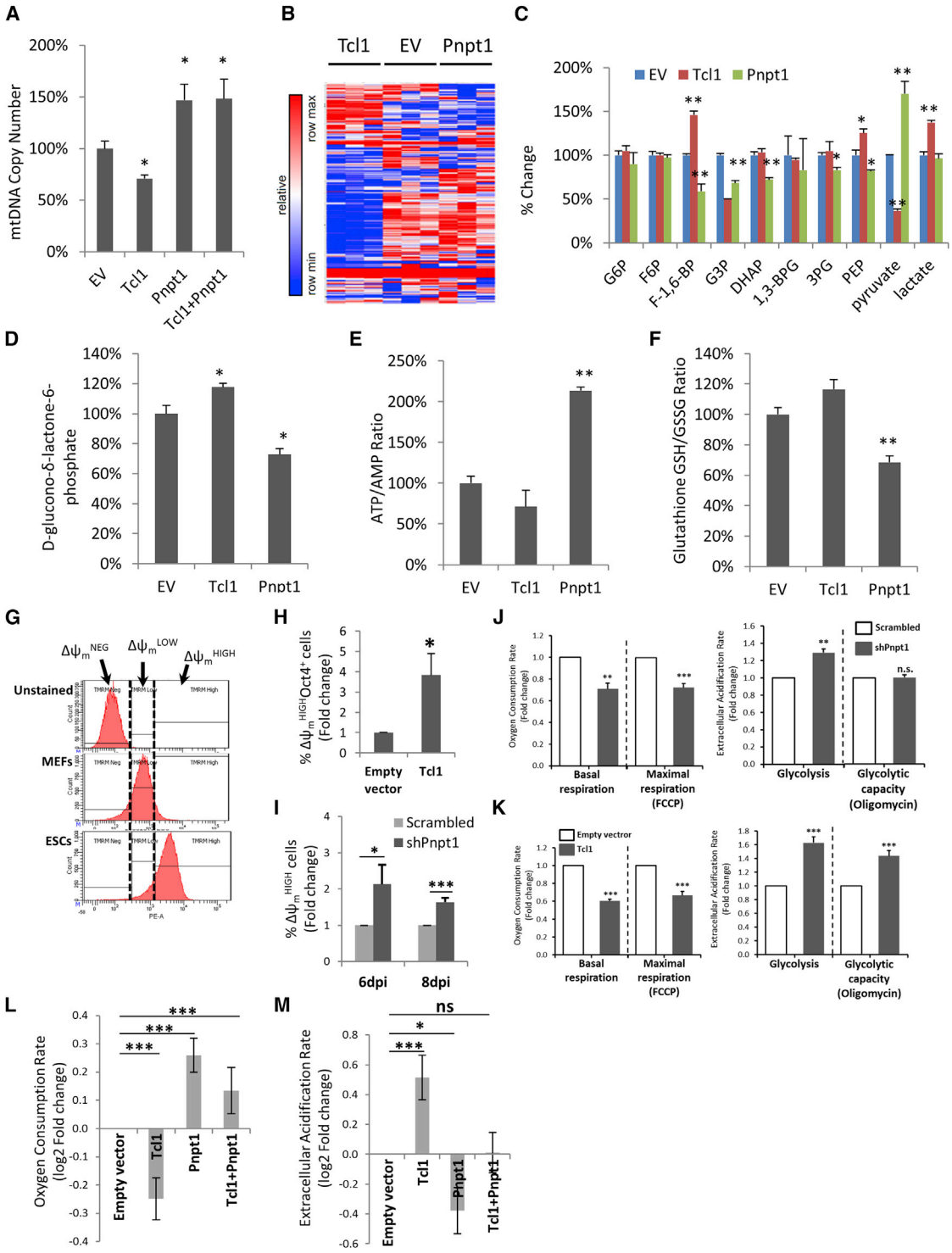

Figure 4. Tcl1-PnPase Pathway Remodels the Cellular Metabolome during Reprogramming

(A) Relative mtDNA copy number after *Tcl1* and *Pnpt1* overexpression in MEFs, relative to the empty vector (EV) control.

(B) Heatmap of metabolite levels, as measured by LC-MS/MS metabolomics in MEFs after overexpression of *Tcl1* and *Pnpt1*, relative to the EV control.

(C) Percent change in glycolysis intermediate levels in MEFs after overexpression of *Tcl1* and *Pnpt1*, relative to the EV control.

(D) Percent change in D-glucono-δ-lactone-6-phosphate levels in MEFs after overexpression of *Tcl1* and *Pnpt1*, relative to the EV control.

(E) Percent change in the ATP/AMP ratio in MEFs after overexpression of *Tcl1* and *Pnpt1*, relative to the EV control.

(F) Percent change in the GSH/GSSG ratio in MEFs after overexpression of *Tcl1* and *Pnpt1*, relative to the EV control.

(legend continued on next page)

the oocyte-enriched Tcl1 and Tcl1b1 proteins enhance reprogramming of iPSCs. Furthermore, we established that Tcl1b1 promotes Akt activation, whereas Tcl1 suppresses mitochondrial PnPase localization in order to promote reprogramming. As shown previously, mitochondrial PnPase serves to promote mitochondrial biogenesis and homeostasis (Chen et al., 2006; Wang et al., 2010a). This supports our observations that the Tcl1-PnPase mechanism operates as a metabolic switch to remodel the cellular metabolome during reprogramming. Furthermore, our genetic experiments with *Tcl1* and *Pnpt1* perturbation in WT versus *p53*$^{-/-}$ backgrounds suggest that the *Tcl1-Pnpt1* switch regulates metabolic reprogramming independently of effects on cellular proliferation and senescence. In fact, *Tcl1* is directly activated by *Oct4* and *Stat3* (Matoba et al., 2006).

Given that we explored the mechanistic basis for the iPSC reprogramming enhancement by the Tcl1 oocyte factors, we initially focused on Akt since it is a well-established binding target of Tcl1 (Laine et al., 2000). We found that Akt phosphorylation increased during iPSC reprogramming and that Akt signaling was both necessary and sufficient for iPSC reprogramming. While we found that both *Tcl1* and *Tcl1b1* enhanced Akt activity, *Tcl1b1* was a significantly more potent Akt activator. Consistently, we found that *Tcl1b1*-overexpressing cells were much more sensitive to Akt inhibition than *Tcl1*-overexpressing cells during reprogramming. Previous studies had also shown that *Tcl1* only modestly increases Akt activation in lymphoma cells (Hoyer et al., 2002). Therefore, it seems that *Tcl1b1* is a more potent Akt coactivator, activating the proliferative and metabolic pathways downstream of Akt to boost reprogramming. In fact, a previous study had shown that a small molecule agonist of the PI3K-PDK1-Akt pathway can also boost reprogramming by upregulating glycolysis (Zhu et al., 2010).

For *Tcl1*, which did not seem as dependent on PI3K-Akt signaling as *Tcl1b1*, we found instead that the mitochondrial RNA-binding PnPase is the relevant binding target of Tcl1 during reprogramming. While total PnPase levels were unaffected by Tcl1, the mitochondrial fraction of PnPase was significantly reduced by overexpression of Tcl1, indicating that Tcl1 suppresses PnPase's mitochondrial localization. Suppression of mitochondrial PnPase by RNAi also significantly enhanced iPSC reprogramming. Through genetic epistasis experiments, we established that PnPase is the downstream target of Tcl1 in remodeling the metabolome during reprogramming.

PnPase regulates RNA import and processing in the mitochondria, which are complex processes crucial for mitochondrial biogenesis and homeostasis (Wang et al., 2010a). Although the multitude of RNAs that are transiently processed by PnPase remains difficult to elucidate, PnPase-mediated import of the *MRP* and *RNase P* RNAs, *5S* rRNA, and tRNAs is known to be essential for mtDNA replication and biogenesis (Wang et al., 2010a). Indeed, cells depleted of *Pnpt1* are known to have less mitochondrial biogenesis and activity (Wang et al., 2010a), consistent with our observations. This is also consistent with others' observations of lower mitochondrial biogenesis and activity in pluripotent stem cells (Prigione et al., 2010; Folmes et al., 2011; Liu et al., 2013). As a regulator of mitochondrial homeostasis, we found that Tcl1-PnPase regulates mitochondrial OxPhos, the ATP/AMP ratio, the redox balance, and, thus, the glycolytic flux. In particular, Tcl1-PnPase also regulates the increased PFK flux and decreased PK flux observed during the glycolytic switch in iPSC reprogramming (Zhu et al., 2010; Shyh-Chang et al., 2013a; Prigione et al., 2010). Thus, the Tcl1-PnPase mechanism serves as a metabolic switch that is capable of remodeling the metabolome during reprogramming. Given this important role in regulating mitochondrial homeostasis, it is unsurprising that PnPase is required for mouse embryogenesis, muscle, brain, and inner ear development (Wang et al., 2010a; Vedrenne et al., 2012; von Ameln et al., 2012). Since mitochondrial numbers and functions are also tightly regulated in pre-fertilization oocytes and early embryonic development (Shyh-Chang et al., 2013b), the Tcl1-PnPase switch might be relevant not only for regulating mitochondria in iPSC reprogramming but also for mitochondrial replacement in aged oocytes and during in vitro fertilization.

EXPERIMENTAL PROCEDURES

Murine iPSC Reprogramming Assay and Drug Treatment

Reprogramming of primary MEFs was performed according to previously published protocols (Takahashi and Yamanaka, 2006).

Protein Extraction and Western Blotting

Cells were harvested and processed according to previously published protocols (Shyh-Chang et al., 2013a). Immunoblot membranes were probed with specific antibodies: GAPDH, (Santa Cruz Biotechnology, SC137179), PnPase (Santa Cruz, SC365049), Akt (Cell Signaling Technology, #9272), phosphoAkt1 (Ser473) (Cell Signaling Technology, #4060), Tim13A/B (Santa Cruz, SC17065), and HA (Covance MMS-101P). Antibody-protein complexes were detected by horseradish peroxidase (HRP)-conjugated antibodies and ECL-Plus (Amersham Biosciences).

Oxygen Consumption and Extracellular Flux Measurement

Infected MEFs were seeded onto Seahorse assay plates (pre-coated with 0.1% gelatin) at 15,000 cells per well 1 day before the assay. We replaced culture media with assay media (Seahorse Bioscience) 1 hr before data collection using the XFe96 Seahorse analyzer. Glucose (Sigma-Aldrich; final concentration, 25 mM), oligomycin (Sigma-Aldrich; final concentration, 1 μM), FCCP (Sigma-Aldrich; final concentration, 1 μM), and a mixture of antimycin and rotenone (Sigma-Aldrich; final concentration, 1 μM) were injected sequentially

(G) TMRM intensity distributions of stained ESCs and MEFs, relative to unstained cells.
(H) Percentage of $\Delta\psi_m^{HIGH}$ cells after *Tcl1* overexpression during OSK-mediated reprogramming of WT MEFs.
(I) Percentage of $\Delta\psi_m^{HIGH}$ cells after shRNA knockdown of *Pnpt1* relative to scrambled control at 6 days (6 dpi) or 8 days (8 dpi) post-induction of OSK-mediated reprogramming of WT MEFs.
(J) OCR and ECAR after *Pnpt1* shRNA knockdown, relative to scrambled control.
(K) OCR and ECAR after *Tcl1* overexpression, relative to empty vector control.
(L and M) Here, (L) OCR and (M) ECAR after co-overexpression of *Tcl1* and *Pnpt1* in MEFs are shown, relative to empty vector control. Fold changes were plotted in $\log_2$ scale to capture both the efficiency gains and losses adequately.
All data are shown as the mean ± SEM of at least three biological replicates. *$p < 0.05$; **$p < 0.01$; ***$p < 0.001$; ns, not significant. See also Figure S5 and Table S1.

during measurement for bioenergetics profile analysis. Measurements were taken according to manufacturer's instructions.

Targeted LC-MS/MS

LC-MS/MS was performed according to previously published protocols (Shyh-Chang et al., 2013a).

For detailed materials and procedures, please see the Supplemental Experimental Procedures.

SUPPLEMENTAL INFORMATION

Supplemental Information includes Supplemental Experimental Procedures, four figures, and two tables and can be found with this article online at http://dx.doi.org/10.1016/j.celrep.2015.07.032.

ACKNOWLEDGMENTS

We are grateful to Nichane Massimo, Siming Ma, and Kyle M. Loh for discussion and critical reading of the paper. Thanks to John Asara, Min Yuan, Nicole Lim Tao Ying, and Khairulanwar Bin Ismail for technical assistance. This work was supported by the Singapore Agency for Science, Technology, and Research (A*STAR), the Genome Institute of Singapore, and the National Research Foundation, Singapore. B.L. is currently based at the Merck Research Laboratories, Translational Medicine Research Centre, Singapore.

Received: June 10, 2015
Revised: July 9, 2015
Accepted: July 15, 2015
Published: August 6, 2015

REFERENCES

Brambrink, T., Hochedlinger, K., Bell, G., and Jaenisch, R. (2006). ES cells derived from cloned and fertilized blastocysts are transcriptionally and functionally indistinguishable. Proc. Natl. Acad. Sci. USA *103*, 933–938.

Buganim, Y., Faddah, D.A., Cheng, A.W., Itskovich, E., Markoulaki, S., Ganz, K., Klemm, S.L., van Oudenaarden, A., and Jaenisch, R. (2012). Single-cell expression analyses during cellular reprogramming reveal an early stochastic and a late hierarchic phase. Cell *150*, 1209–1222.

Chen, H.-W., Rainey, R.N., Balatoni, C.E., Dawson, D.W., Troke, J.J., Wasiak, S., Hong, J.S., McBride, H.M., Koehler, C.M., Teitell, M.A., and French, S.W. (2006). Mammalian polynucleotide phosphorylase is an intermembrane space RNase that maintains mitochondrial homeostasis. Mol. Cell. Biol. *26*, 8475–8487.

Fantin, V.R., St-Pierre, J., and Leder, P. (2006). Attenuation of LDH-A expression uncovers a link between glycolysis, mitochondrial physiology, and tumor maintenance. Cancer Cell *9*, 425–434.

Folmes, C.D., Nelson, T.J., Martinez-Fernandez, A., Arrell, D.K., Lindor, J.Z., Dzeja, P.P., Ikeda, Y., Perez-Terzic, C., and Terzic, A. (2011). Somatic oxidative bioenergetics transitions into pluripotency-dependent glycolysis to facilitate nuclear reprogramming. Cell Metab. *14*, 264–271.

Golipour, A., David, L., Liu, Y., Jayakumaran, G., Hirsch, C.L., Trcka, D., and Wrana, J.L. (2012). A late transition in somatic cell reprogramming requires regulators distinct from the pluripotency network. Cell Stem Cell *11*, 769–782.

Gurdon, J.B., and Melton, D.A. (2008). Nuclear reprogramming in cells. Science *322*, 1811–1815.

Hallas, C., Pekarsky, Y., Itoyama, T., Varnum, J., Bichi, R., Rothstein, J.L., and Croce, C.M. (1999). Genomic analysis of human and mouse TCL1 loci reveals a complex of tightly clustered genes. Proc. Natl. Acad. Sci. USA *96*, 14418–14423.

Han, J., Yuan, P., Yang, H., Zhang, J., Soh, B.S., Li, P., Lim, S.L., Cao, S., Tay, J., Orlov, Y.L., et al. (2010). Tbx3 improves the germ-line competency of induced pluripotent stem cells. Nature *463*, 1096–1100.

Hoyer, K.K., French, S.W., Turner, D.E., Nguyen, M.T., Renard, M., Malone, C.S., Knoetig, S., Qi, C.F., Su, T.T., Cheroutre, H., et al. (2002). Dysregulated TCL1 promotes multiple classes of mature B cell lymphoma. Proc. Natl. Acad. Sci. USA *99*, 14392–14397.

Laine, J., Künstle, G., Obata, T., Sha, M., and Noguchi, M. (2000). The protooncogene TCL1 is an Akt kinase coactivator. Mol. Cell *6*, 395–407.

Le, R., Kou, Z., Jiang, Y., Li, M., Huang, B., Liu, W., Li, H., Kou, X., He, W., Rudolph, K.L., et al. (2014). Enhanced telomere rejuvenation in pluripotent cells reprogrammed via nuclear transfer relative to induced pluripotent stem cells. Cell Stem Cell *14*, 27–39.

Liu, W., Long, Q., Chen, K., Li, S., Xiang, G., Chen, S., Liu, X., Li, Y., Yang, L., Dong, D., et al. (2013). Mitochondrial metabolism transition cooperates with nuclear reprogramming during induced pluripotent stem cell generation. Biochem. Biophys. Res. Commun. *431*, 767–771.

Matoba, R., Niwa, H., Masui, S., Ohtsuka, S., Carter, M.G., Sharov, A.A., and Ko, M.S. (2006). Dissecting Oct3/4-regulated gene networks in embryonic stem cells by expression profiling. PLoS ONE *1*, e26.

Nakamura, T., Inoue, K., Ogawa, S., Umehara, H., Ogonuki, N., Miki, H., Kimura, T., Ogura, A., and Nakano, T. (2008). Effects of Akt signaling on nuclear reprogramming. Genes Cells *13*, 1269–1277.

Niwa, H., Ogawa, K., Shimosato, D., and Adachi, K. (2009). A parallel circuit of LIF signalling pathways maintains pluripotency of mouse ES cells. Nature *460*, 118–122.

Prigione, A., Fauler, B., Lurz, R., Lehrach, H., and Adjaye, J. (2010). The senescence-related mitochondrial/oxidative stress pathway is repressed in human induced pluripotent stem cells. Stem Cells *28*, 721–733.

Shyh-Chang, N., Locasale, J.W., Lyssiotis, C.A., Zheng, Y., Teo, R.Y., Ratanasirintrawoot, S., Zhang, J., Onder, T., Unternaehrer, J.J., Zhu, H., et al. (2013a). Influence of threonine metabolism on S-adenosylmethionine and histone methylation. Science *339*, 222–226.

Shyh-Chang, N., Daley, G.Q., and Cantley, L.C. (2013b). Stem cell metabolism in tissue development and aging. Development *140*, 2535–2547.

Silva, J., Nichols, J., Theunissen, T.W., Guo, G., van Oosten, A.L., Barrandon, O., Wray, J., Yamanaka, S., Chambers, I., and Smith, A. (2009). Nanog is the gateway to the pluripotent ground state. Cell *138*, 722–737.

Stadtfeld, M., and Hochedlinger, K. (2010). Induced pluripotency: history, mechanisms, and applications. Genes Dev. *24*, 2239–2263.

Takahashi, K., and Yamanaka, S. (2006). Induction of pluripotent stem cells from mouse embryonic and adult fibroblast cultures by defined factors. Cell *126*, 663–676.

Vedrenne, V., Gowher, A., De Lonlay, P., Nitschke, P., Serre, V., Boddaert, N., Altuzarra, C., Mager-Heckel, A.M., Chretien, F., Entelis, N., et al. (2012). Mutation in PNPT1, which encodes a polyribonucleotide nucleotidyltransferase, impairs RNA import into mitochondria and causes respiratory-chain deficiency. Am. J. Hum. Genet. *91*, 912–918.

von Ameln, S., Wang, G., Boulouiz, R., Rutherford, M.A., Smith, G.M., Li, Y., Pogoda, H.M., Nürnberg, G., Stiller, B., Volk, A.E., et al. (2012). A mutation in PNPT1, encoding mitochondrial-RNA-import protein PNPase, causes hereditary hearing loss. Am. J. Hum. Genet. *91*, 919–927.

Wang, G., Chen, H.W., Oktay, Y., Zhang, J., Allen, E.L., Smith, G.M., Fan, K.C., Hong, J.S., French, S.W., McCaffery, J.M., et al. (2010a). PNPASE regulates RNA import into mitochondria. Cell *142*, 456–467.

Wang, S., Kou, Z., Jing, Z., Zhang, Y., Guo, X., Dong, M., Wilmut, I., and Gao, S. (2010b). Proteome of mouse oocytes at different developmental stages. Proc. Natl. Acad. Sci. USA *107*, 17639–17644.

Yoshida, Y., Takahashi, K., Okita, K., Ichisaka, T., and Yamanaka, S. (2009). Hypoxia enhances the generation of induced pluripotent stem cells. Cell Stem Cell *5*, 237–241.

Zhang, P., Ni, X., Guo, Y., Guo, X., Wang, Y., Zhou, Z., Huo, R., and Sha, J. (2009). Proteomic-based identification of maternal proteins in mature mouse oocytes. BMC Genomics *10*, 348.

Zhu, S., Li, W., Zhou, H., Wei, W., Ambasudhan, R., Lin, T., Kim, J., Zhang, K., and Ding, S. (2010). Reprogramming of human primary somatic cells by OCT4 and chemical compounds. Cell Stem Cell *7*, 651–655.